Hindawi
International Journal of Polymer Science
Volume 2018, Article ID 7823587, 9 pages
https://doi.org/10.1155/2018/7823587

Research Article

Preparation and Application in Drug Storage and Delivery of Agarose Nanoparticles

Pablo G. Argudo,[1] Eduardo Guzmán,[1,2] Alejandro Lucia,[3] Ramón G. Rubio,[1,2] and Francisco Ortega[1,2]

[1]*Departamento de Química Física I, Universidad Complutense de Madrid, Ciudad Universitaria s/n, 28040 Madrid, Spain*
[2]*Instituto Pluridisciplinar, Universidad Complutense de Madrid, Paseo Juan XXIII 1, 28040 Madrid, Spain*
[3]*Instituto de Ecología y Desarrollo Sustentable (INEDES, CONICET-UNLu), Ruta 5 y Avenida Constitución, 6700 Luján, Buenos Aires, Argentina*

Correspondence should be addressed to Eduardo Guzmán; eduardogs@quim.ucm.es and Francisco Ortega; fortega@quim.ucm.es

Received 10 July 2018; Revised 20 September 2018; Accepted 13 November 2018; Published 19 December 2018

Academic Editor: Angel Concheiro

In this work, monodisperse agarose gel nanoparticles were prepared using a W/O microemulsion as a template to control the size of the obtained particles. The combination of this template method with a temperature-induced gelling and a solvent exchange methodology has allowed preparing stable aqueous dispersions of monodisperse agarose gel nanoparticles in water. The average size, measured as an apparent hydrodynamic diameter, of the obtained particles was around 150 nm. The ability of the obtained hydrogel particles for the encapsulation and release of a synthetic insecticide (azamethiphos) was tested. The results evidence that the insecticide molecules encapsulated in the fabricated nanoparticles are released following a diffusion-controlled mechanism. These results combined with the biodegradability of the agarose provide the bases for the design of a new vector with application in the control of parasites in water reservoirs.

1. Introduction

Encapsulation of active ingredients has become a multidisciplinary challenge with interest in several industries, e.g., pharmaceutical, medical, cosmetics, chemical, food, and agricultural [1–9]. This is mainly because encapsulation creates a barrier to protect encapsulated compounds (liquid, solid, and gas) that allows isolating them from the surrounding environment, thus avoiding their degradation and oxidation during its storage and limiting their interactions and reactions with other compounds. Therefore, encapsulation provides the bases for increasing the shelf life of the encapsulated compounds, especially those extremely labile. This enhances its stability and allows one to control the release process without modification of the encapsulated compound activity [10, 11]. Even though the development of encapsulation methodologies started in the last '50s of the last century [12], it was not until the last two decades when the progresses on the nanoscience and nanoengineering have allowed the development of efficient and reproducible encapsulation methodologies, lowering costs and enabling the industrial production [13, 14].

Many different nano- and microstructured supramolecular systems, e.g., colloidal particles, liposomes, and micelles, have been used on the development of efficient encapsulation platforms. Among such systems, biopolymer matrices are accounted as one of the most successful due to their availability, low cost, and reduced impact on the environment and human health [15, 16]. Furthermore, many different biopolymers, either proteins or polysaccharides, are frequently used on the fabrication of particles, e.g., whey and soy proteins, casein, gelatin, zein, starch, cellulose, chitosan, and alginate [17]. These particles are classified into three main groups depending on their structure: hydrogels,

inclusion complexes, and interpolyelectrolyte complexes. This leads to the existence of particles with a broad range of physicochemical and functional attributes. It is also important that particles can be obtained following different methodologies (molding techniques, spray drying, solvent desorption, injection and microfluidic and shearing methods, and emulsion-templating methods) [18]. The choice of the most adequate system for a certain purpose and the methodology used for its preparation depends on different factors, e.g., properties of desired particles and biopolymers and the nature of the material to be encapsulated. In addition, the methodology used for the fabrication of the encapsulation platforms must be easy and cost effective [19].

A successful approach for fabricating biopolymer particles is the use of the emulsion templating method which relies on the use of drops of water in oil (W/O) emulsions as a template for the fabrication of the particles [18]. For this purpose, an aqueous solution of the biopolymer is homogenized with an oil solution containing a surfactant, thus leading to the formation of a W/O emulsion. The size of the drop can be controlled by tuning the mixture composition or the homogenization velocity. Once the emulsion is obtained, the water drops are gelled following a specific mechanism, either physical (temperature change) or chemical (pH change, addition of a cross-linking agent), depending on the nature of the biopolymer. The last step of the preparation process involves the solvent exchange process to obtain an aqueous dispersion of biopolymer particles [18]. This methodology has been successfully applied for preparing alginate nanoparticles and mixed nanoparticles of alginate and whey protein [20, 21]. The latter two were successfully used in the encapsulation of riboflavin [21]. Milk protein particles used for probiotic bacteria encapsulation have been also prepared using this methodology [22].

This work is focused on the preparation of agarose nanoparticles. Agarose is a polysaccharide frequently used in different biotechnological applications due to its natural, biodegradable, and nontoxic character which enables the formation of inert nanoparticles. In recent years, an extensive research on polysaccharide nanoparticles for several applications has been developed [23, 24]. Among such polysaccharides, the use of agarose for the fabrication of nanoparticles is widely extended [25, 26]. Wang and Wu [26] described the fabrication of agarose hydrogel nanoparticles using an emulsion-converted-to-suspension method and the application of the obtained particles for encapsulating proteins and peptides. Similar particles were used as batch reactors in dairy industry for the hydrolysis of lactose [27]. Furthermore, many works deal with the fabrication of hybrid metal-agarose particles for combining the electronic properties of metals and the biocompatibility of the agarose to obtain particles with application as biosensors [28, 29].

This work the fabrication of agarose nanoparticles using W/O microemulsions as a template instead of conventional emulsions. The use of microemulsions as a template is preferred due to their thermodynamic stability. Furthermore, drops with sizes in the nanometre scale that provide the bases for fabricating nanosized particles [30]. The aforementioned gelling step takes advantage of the thermal behavior of agarose which presents a gelling temperature of 35–52°C and melting temperature of 85–90°C [31, 32]. Thus, the preparation of W/O with solubilized agarose in the vicinity of the agarose melting followed by a cooling down of the mixture to room temperature, leads to the formation of agarose hydrogel nanoparticles, which after solvent evaporation can be transferred to water and used as a platform for encapsulation of a synthetic insecticide (azamethiphos). Azamethiphos is an insecticide for urban, domestic, or agricultural use, and their encapsulation and controlled release can provide the bases for controlling external parasites in water reservoirs [33].

2. Material and Methods

2.1. Chemicals. Dioctyl sulfosuccinate sodium salt (aerosol-OT, purity ≥ 99.0%), KCl BioXtra (purity ≥ 99.0%), and azamethiphos (S-[(6-chloro-2-oxo[1,3]oxazolo[4,5-b]pyridin-3(2H)-yl)methyl] O,O-dimethyl phosphorothioate) were purchased from Sigma-Aldrich (Germany). n-Heptane (purity > 99%, extra dry) and ultrapure agarose were purchased from Acros Organics (Belgium) and Invitrogen (United States of America), respectively. All the reagents were used as received without further purification.

All the used glassware was cleaned with a saturated solution of KOH in ethanol, followed by rinsing with abundant water. Milli-Q grade water obtained using a multicartridge purification system aquaMAX™ Ultra 370 Series (YoungLin Instrument Co. Ltd., South Korea) was used for rinsing the glassware and for solution preparation. This water obtained presents a resistivity at around 18 MΩ·cm^{-1} and a total organic content lower than 6 ppb.

2.2. Preparation of Agarose Nanoparticles. A three-step method was followed for preparing agarose nanoparticles. The first step involves the preparation of water in oil (W/O) microemulsions that are used as a template to control the size distribution of the particles. The microemulsions were prepared using the ternary system n-heptane/aerosol-OT/water because it is a well-known system and its phase diagram has been extensively studied in the literature [34, 35]. The chosen template microemulsions were composed by 80 wt% of n-heptane, 10 wt% of aerosol-OT, and 10 wt% of water [36]. Once the composition is chosen, the required amount water phase containing an agarose volume fraction of 1% and a KCl concentration of 50 mM is dropped into the organic phase containing n-heptane and aerosol-OT under continuous stirring at 2500 rpm. It is worth mentioning that the aqueous solution of agarose needs to be preheated at 95°C (above the agarose melting temperature) to ensure agarose solubilization. The second step involves the gelling of the microemulsion drops to obtain agarose gel particles dispersed in n-heptane. For this step, the obtained W/O is cooling down at room temperature maintaining the stirring. To obtain a dispersion of agarose gel particles in water, the n-heptane was evaporated by freeze drying and the obtained powder was stored overnight at 4°C. This powder

was redispersed in water leading to a stable aqueous dispersion of agarose gel particles. It is worth mentioning that during the solvent exchange process, some aggregates are obtained. To remove such aggregates and possible residues of aerosol-OT, the dispersion of gel particles was filtered using nylon membranes with a pore diameter of 0.45 μm (Millipore, United States of America) followed by dialysis during 8 hours of the filtered samples using membranes with a molecular weight cut-off of 12 kDa. The result is a stable aqueous dispersion of monodisperse agarose gel nanoparticles.

Once the process of gel particles was optimized, they were used for azamethiphos encapsulation. For this purpose, a concentration of 0.01 mM of the drug was added to the initial aqueous phase used for the microemulsion preparation.

2.3. Experimental Techniques. The apparent size of the gel particles was estimated as the apparent hydrodynamic diameter d_h^{app}, using dynamic light scattering (DLS) measurements. For this purpose, a Zetasizer Nano ZS instrument (Malvern Instruments Ltd., Worcestershire, UK) was used. DLS experiments were performed in quasibackscattering configuration (scattering angle, $\theta = 173^\circ$) using radiation of the red line of a He-Ne laser (wavelength, $\lambda = 633$ nm). Before the measurements, samples were filtered, in a clean room, using nylon membranes with a pore diameter of 0.45 μm (Millipore, United States of America). Thus, it is possible to remove dust particles from the samples. The measurements were carried out using optical glass cell (Hellma®6030-OG Model; Hellma, Jena, Germany). In DLS experiments, the normalized intensity autocorrelation function, $g^{(2)}(q,t)$, follows an exponential decay with time. In the simplest case that considers the Brownian motion of monodisperse scatterers, $g^{(2)}(q,t)$ is defined as follows:

$$g^{(2)}(q,t) - 1 = \beta e^{-t/\tau} = \beta e^{-D_{app}q^2 t}, \quad (1)$$

where t represents the time, τ is the characteristic relaxation time which is directly related to the apparent diffusion coefficient D_{app}, $q = (4\pi n/\lambda)\sin(\theta/2)$ is the wavevector, n is the solution refractive index which was assumed to be close to that of the continuous phase ($n = 1.33$ and $n = 1.39$ for water and n-heptane, respectively), and β, which is close to 1, is the coherence factor. For spherical particles diffusing in a continuous Newtonian medium, $D_{app} = 1/\tau q^2$ can be assumed to follow the Stoke-Einstein relationship allowing for determining the apparent hydrodynamic diameter:

$$D_{app} = \frac{k_B T}{3\pi\eta d_h^{app}}, \quad (2)$$

where k_B and T are the Boltzmann constant and the absolute temperature, respectively, and η is the viscosity of the continuous phase.

Information on the surface charge of the dispersed particles was also obtained using the Zetasizer Nano ZS instrument (Malvern Instruments Ltd., Worcestershire, UK). For this purpose, electrophoretic mobility (μ_e) measurements were carried out. The measured μ_e values were transformed into ζ-potential using Smoluchowski's relationship.

Studies about the encapsulation and release of azamethiphos from nanoparticles were performed by spectroscopic measurements. UV-visible spectroscopy measurements were performed using an UV-visible diode spectrophotometer model HP-8452a (Hewlett-Packard, United States of America), and fluorescence measurements were carried out using a fluorescence spectrophotometer FP-6500 (JASCO Inc., United States of America).

3. Results and Discussion

3.1. Agarose Nanoparticle Preparation. The preparation of agarose gel nanoparticles involves the use of W/O microemulsions as a template; thus, the first step of our study involves the study of the size of the water drops of the bare microemulsion stabilized with aerosol-OT (composition: 80 wt% n-heptane, 10 wt% aerosol-OT, and 10 wt% water). Figure 1(a) shows the intensity autocorrelation function obtained for the bare microemulsion measurements.

The autocorrelation function for water drops presents a monomodal character which is clearer from the d_h^{app} distribution (Figure 1(b)). The d_h^{app} distribution for the water drops in n-heptane is relatively narrow (polydispersity index, PDI < 0.1), appearing centered at around 15 nm. When the results obtained for the W/O microemulsions are compared with those obtained for the agarose nanoparticles after gelling, no significant changes were found neither on the intensity autocorrelation function (Figure 1(a)) nor on the d_h^{app} distribution (Figure 1(b)). These results evidence that the use of W/O microemulsions as a template for preparing agarose gel nanoparticles allows controlling the size of the obtained particles; i.e., the size of the gel nanoparticles is similar to that of the water drops of the O/W microemulsion used as a template. The nanoparticles obtained in n-heptane had an average d_h^{app} at around 12 nm.

In spite of the success on the preparation of monodisperse agarose gel particles in n-heptane, the application of such particles in technological relevant applications requires transferring the obtained particles to an eco-friendly solvent such as water. This process was carried out by freeze drying evaporation of the n-heptane followed by redispersion of the obtained powder in water. Figure 2 shows the intensity autocorrelation function and the d_h^{app} distribution obtained for the particles after redispersion in water.

The results show that the monomodal character of the intensity autocorrelation function (Figure 2(a)) is lost during the evaporation of the n-heptane and the subsequent redispersion in water of the agarose particle and at least three well-separated components can be identified in the sample. The characteristic diffusion times for such processes are around 1 μs, 10–100 μs, and 0.1 s. This evidences that the preparation process of the nanoparticles leads to a rather polydisperse dispersion of nanoparticles. The d_h^{app} distribution obtained from the analysis of the intensity autocorrelation function confirms the existence of three different

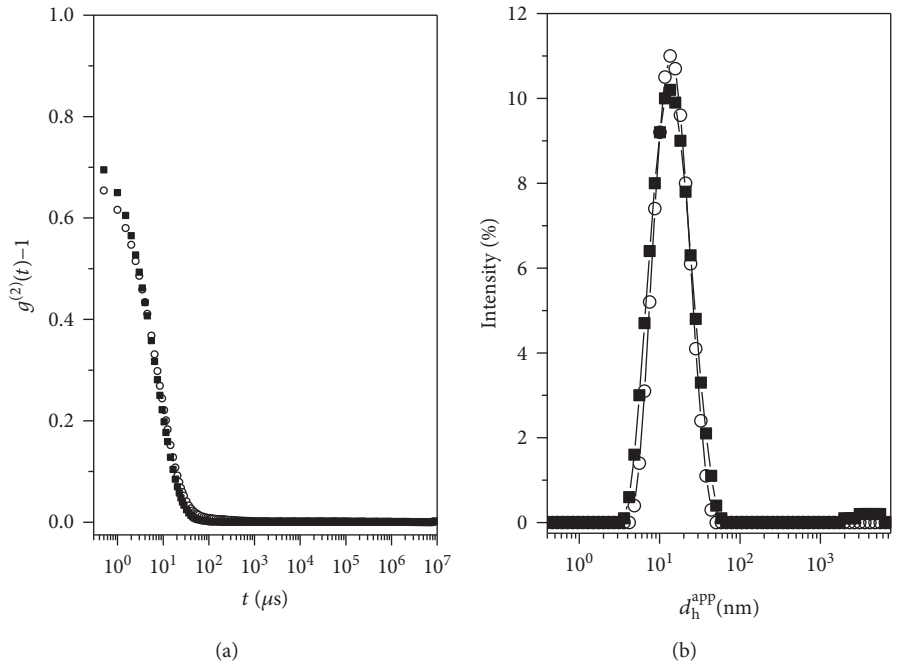

Figure 1: (a) Intensity autocorrelation functions as were obtained from DLS experiments for water drops in the template W/O microemulsion (○) and for agarose particles as were obtained in n-heptane (■). (b) d_h^{app} distributions obtained from the analysis of the intensity autocorrelation function in (a) for water drops in the template W/O microemulsion (○) and for agarose particles as were obtained in n-heptane (■).

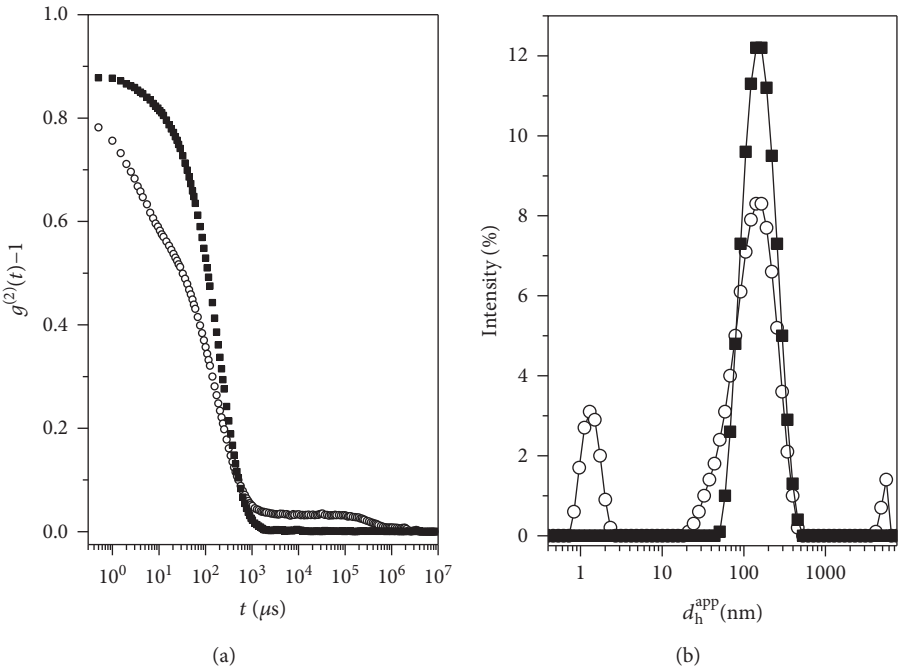

Figure 2: (a) Intensity autocorrelation functions as were obtained from DLS experiments for agarose gel particles in water after resuspension (○) and for agarose gel particles in water after the cleaning process (■). (b) d_h^{app} distributions obtained from the analysis of the intensity autocorrelation function in (a) for agarose gel particles in water after resuspension (○) and for agarose gel particles in water after the cleaning process (■).

populations afterward the solvent exchange and subsequent redispersion of the agarose particles in water. The first population can be ascribed to micelles of the aerosol-OT used in the stabilization of the microemulsion. Aerosol-OT is also soluble in water; thus, it can be expected that a part of it can remain as free surfactant and above the critical micelle concentration (cmc) as micelles upon redispersion [37]. The second population is associated with the obtained agarose particles which present an average d_h^{app} at around 150 nm. This evidences that the average size of the particles in water is tenfold of the one previously found in n-heptane. This swelling process occurring during the solvent exchange process can be explained assuming that n-heptane is not a good solvent for agarose; thus, nanoparticles remain in a collapsed state to minimize the number of contacts with the nonpolar phase. However, the dispersion of nanoparticles in water leads to the swelling of the agarose matrix because water is a good solvent for agarose. This justifies the increase of the particle size to its final value [38, 39]. The last population found is related to the formation of particle aggregates during the exchange solvent process. However, it is worth noting that the importance of this last population can be considered negligible in comparison to the contributions of the population centered at around 150 nm.

The technological application of the obtained agarose particles requires removing from aqueous suspension both free surfactant and aggregate molecules. The latter two (aggregates with sizes larger than 1 μm) are easily removed by filtration of the dispersions through a nylon membrane with a pore diameter of around 0.45 μm. In order to remove the excess of free aerosol-OT, the agarose particle dispersions were subjected to dialysis against pure water during 8 hours. This time was found to be enough to obtain a dispersion of particles in which there are neither free surfactant molecules nor particle aggregates. The study of such dispersion using DLS (see Figure 2) evidences the presence of rather monodisperse gel particles with an average d_h^{app} centered at around 140 nm (PDI < 0.1). It is worth mentioning that the obtained gel particles present a good stability in aqueous medium due to its high negative charge as was found by ζ-potential measurements. In the particular case of the here-studied particles, its ζ-potential was (-74 ± 3) mV. This negative charge is explained considering that during the particle preparation, a shell of aerosol-OT remains attached onto the surface of the particles, providing electrostatic stability to the nanoparticles and minimizing the aggregation phenomena. Table 1 summarizes the main characteristics of the obtained particles.

3.2. Thermoresponsiveness of Gel Nanoparticles. It is well known that agarose presents a sol-gel transition around human physiological temperature (37°C). The sol-gel transition is strongly dependent on the length of agarose chains and the cross-linking degree of the polymer network [32, 40] Thus, it is expected that the increase of the temperature beyond the transition temperature can lead to a significant change of the nanoparticles size which can be an advantage for applications in which the load and release of active compounds from the gel matrix are required. However, most important than the gel swelling upon the increase of the temperature is the reversibility of such process, i.e., the reversible swelling-shrinking of the gel as result of its subsequent heating and cooling. This section analyses the response of the obtained agarose nanoparticles when they are subjected to an increase of temperature from room temperature to 65°C and after they were cooled down again to room temperature. Figure 3 shows the temperature dependence of the apparent hydrodynamic diameter during the thermal treatment of the nanoparticles.

The results point out that the increase of temperature leads to the swelling of agarose gel nanoparticles until their size reaches a value at 60°C that is twice the original size of nanoparticles in water at room temperature (25°C). The subsequent decrease of temperature down to 25°C leads to the shrinking of the particles till recovering the initial size. This result points out that the agarose gel nanoparticles obtained present a reversible response against temperature changes, without significant hysteresis. The results also show a change on the slope of the dependence of the d_h^{app} in the 35–40°C range which can be explained as a result of the sol-gel transition of agarose. This behavior can be considered an advantage to trigger the release of active compounds from nanoparticles to human body [40].

The transition found in the nanoparticles may be explained assuming that as the temperature is approached at the melting temperature of agarose, water becomes a better solvent for nanoparticles. Thus, the here-obtained nanoparticles can be considered a physically cross-linked hydrogel with a lower critical solution temperature (LCST) at around 37°C.

3.3. Encapsulation of Azamethiphos in Gel Nanoparticles. Gel nanoparticles can be used for encapsulation and release of active compounds. Here, the encapsulation and release of a synthetic insecticide (azamethiphos) inside the agarose matrix have been explored. Table 1 summarised the apparent hydrodynamic diameter of agarose nanoparticles without and with encapsulated azamethiphos. The comparison of the results evidences clearly that the inclusion of azamethiphos does not change significantly the particle characteristics (size or surface charge). Thus, it is possible to use agarose nanoparticles as platforms for azamethiphos encapsulation without compromising significantly the physicochemical characteristics of the obtained particles. The evaluation of the degree of retention of azamethiphos during the preparation of the loaded nanoparticles was performed using UV-visible spectroscopy. Figure 4 shows the UV-visible spectrum of azamethiphos in water.

The UV-visible spectrum of azamethiphos in water shows three bands centered at 183, 211, and 274 nm. For the evaluation of the retention degree, we have followed the band at 274 nm in order to avoid overlapping with the absorbance of any other component of the sample. The inserted plot in Figure 4 represents the dependence of the absorbance (A) at 274 on the concentration for azamethiphos solutions in water. The results show a linear dependence of such absorbance on the concentration of the insecticide ($c_{azamethiphos}$) in the studied range (Lambert-Beer law). The molar absorptivity of the azamethiphos obtained

Table 1: Main characteristics of nanoparticles as were obtained dispersed in n-heptane and in water after the solvent exchange process.

	Bare agarose nanoparticles		Agarose nanoparticles loaded with azamethiphos	
	d_h^{app} (nm)	ζ-potential (mV)	d_h^{app} (nm)	ζ-potential (mV)
Dispersion in n-heptane	12 ± 2	—	14 ± 2	—
Dispersion in water	140 ± 10	-74 ± 4	150 ± 20	-70 ± 5

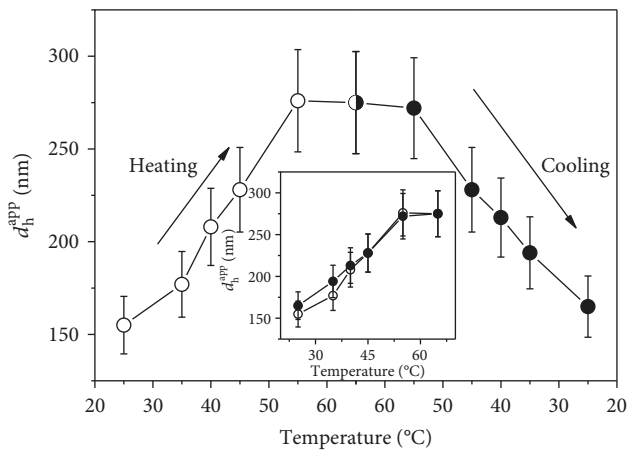

Figure 3: Dependence of the d_h^{app} of agarose gel nanoparticles on the temperature during the heating (○)–cooling (●) cycle. The inserted figure represents the same results of the main panel showing the reversibility of the heating–cooling cycle. The heating–cooling steps were carried out slowly enough (0.25°C/min) to ensure the quasistatic character of the temperature change.

was $1.010 \pm 0.003 \times 10^7\ \mathrm{cm^2 \cdot mol^{-1}}$. From the concentration, dependence of the absorbance it is possible to determine the amount of azamethiphos remaining after the process of preparation of the loaded nanoparticles. The comparison of the UV-visible spectra of agarose solution with azamethiphos before the preparation process with that obtained after the preparation process of nanoparticles with encapsulated azamethiphos allows one to determine the efficiency of the encapsulation process. Figure 5 shows the UV-visible spectra of an agarose aqueous solution including a concentration 0.01 mM of azamethiphos and that of the nanoparticles with encapsulated azamethiphos obtained from the same initial solution. Note that the water volume used for the preparation of the template microemulsion is the same in which the final particles were dispersed. Therefore, in the case that all azamethiphos were encapsulated, the concentrations would be the same and both spectra should overlap.

The decrease of the absorbance evidences that during the preparation process of agarose-loaded nanoparticles, a part of the initial azamethiphos is lost. Thus, the encapsulation process yields efficiency in the 60–70% range of the initial amount of insecticide. This decrease of the azamethiphos concentration during the encapsulation may be probably associated with the amount of azamethiphos that remains trapped in the aggregates of big size that are removed during the solvent exchange process. It is important to note that the solubility of azamethiphos is n-heptane is negligible; thus, the transference of the insecticide to the oil phase during particle preparation can be ruled out.

Once the encapsulation of azamethiphos in the agarose particle is confirmed, the release of the insecticide from particles to the solvent at 25°C was evaluated taking advantage of the fluorescent emission of azamethiphos at 339 nm after excitation at 274 nm. For this purpose, a fresh dispersion of agarose nanoparticles with encapsulated azamethiphos was placed into dialysis tubes and the intensity of fluorescence was evaluated in aliquot of the surrounding water at several times after the preparation of the loaded nanoparticles. For the evaluation of the azamethiphos concentration released to water, a calibration curve was carried out measuring the fluorescence intensity of azamethiphos solutions of different concentrations (see Figure 6). From this calibration curve, it is possible to infer with the existence of a linear dependence of the fluorescence intensity (I) on the azamethiphos concentration within the studied concentration range ($I = Kc_{\mathrm{azamethiphos}}$, where K is an optical constant dependent on the studied process and assumes a value of $6.80 \pm 0.04 \times 10^7$ l/mol). Using the calibration curve, it is possible to evaluate the released amount of azamethiphos from the nanoparticles.

The azamethiphos release kinetics obtained from the fluorescence intensity of the water surrounding our particle dispersion inside the dialysis is represented in terms of the fraction of released azamethiphos in Figure 7. It is worth mentioning that to ensure the homogenization of the concentration of azamethiphos in water during the release process, the aqueous medium was subjected to continuous agitation at 500 rpm.

The release of azamethiphos from agarose gel nanoparticles occurs mainly in the early stages, with a released amount of around the 70% of the initial encapsulated azamethiphos after 15 minutes. Then a sustained release during almost 6 hours occurs till reaching a complete release of the encapsulated azamethiphos. On the basis of the study performed for the release in which temperature was kept constant at room temperature, and assuming that the physicochemical properties of particles do not change significantly with the azamethiphos encapsulation, it is possible to assume that the release of azamethiphos occurs by a diffusion-controlled mechanism through the porous matrix of agarose nanoparticles. An empirical model to describe a diffusion-controlled release of an encapsulated compound from a hydrogel matrix was developed by Peppas et al. [41, 42]. This model described the time

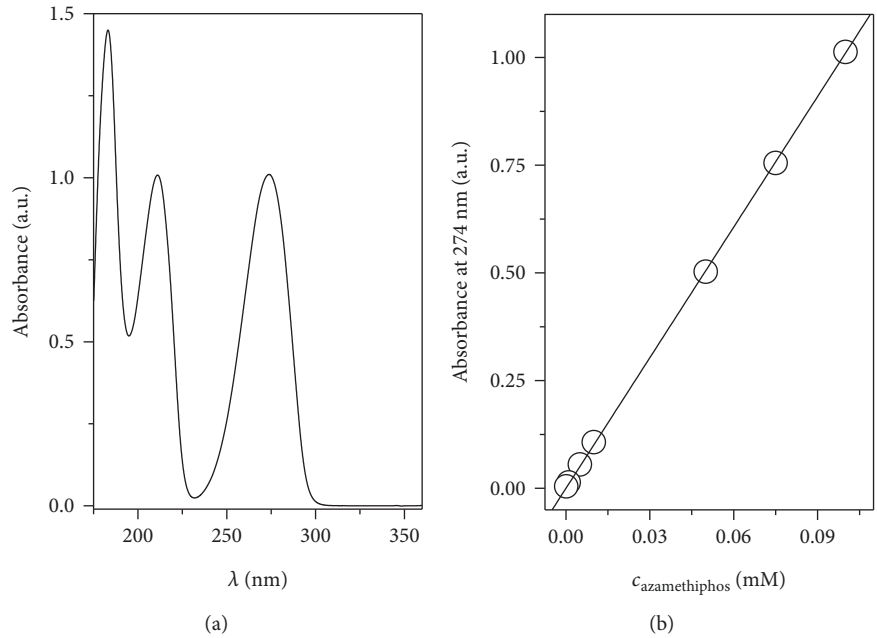

Figure 4: (a) UV-visible spectra of azamethiphos solution in water with 0.1 mM concentration. (b) Experimental dependence of the absorbance at 274 nm on the azamethiphos concentration for solutions of the insecticide in water (symbols) and the fit to the Lambert-Beer law (line).

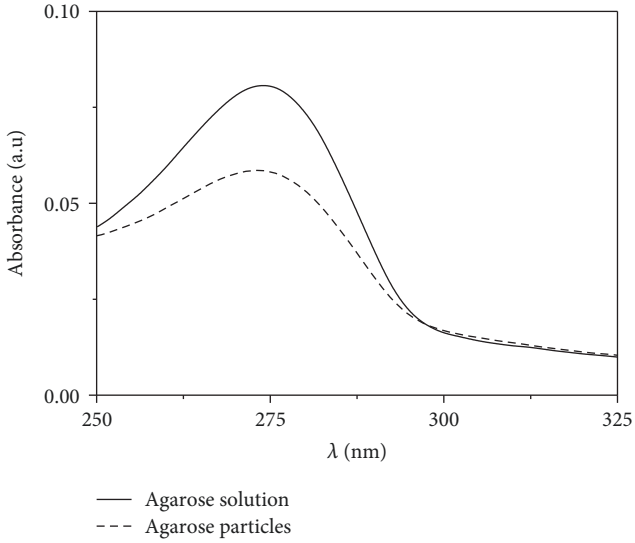

Figure 5: UV-visible spectra of azamethiphos solution in water with 0.01 mM concentration and agarose particles loaded with azamethiphos obtained using the same solution for its preparation.

dependence of the fraction of released compound ϕ as a power law defined as follows:

$$\phi = kt^n, \tag{3}$$

where k is a structural/geometrical constant depending on the particular system and n is the release exponent describing the release mechanism. The experimental data obtained for the release of the encapsulated azamethiphos agrees well with the description provided by the empirical law with the parameters assuming the following values: $k = 0.54 \pm 0.01$ and $n = 0.109 \pm 0.005$. Thus, the results confirm the diffusion-controlled release of azamethiphos from the agarose nanoparticles. Similar diffusion-controlled mechanisms were found by Wang and Wu [26] for the release of ovoalbumin from agarose nanoparticles and by Rekha and Sharma [43] for the release of insulin from chitosan-modified particles. It is worth mentioning that the diffusion-controlled mechanism has been described in the literature as the most extended mechanism for the release of molecules from polysaccharide particles [44].

4. Conclusions

This work presents a new route for preparation of aqueous dispersions of stable and monodisperse nanosized agarose gel nanoparticles. This was possible by the temperature-triggered gelation of the aqueous drops of the W/O microemulsions used as a template for controlling the size and morphology of the nanoparticles. Such nanoparticles can be transferred to aqueous medium to obtain a dispersion of highly charged nanoparticles which present a physicochemical behavior reminiscent of a physically cross-linked gel which can undergo a reversible swelling-shrinking process enabling for a controlled triggering of encapsulated compounds.

The obtained particles can be used for encapsulation of active compounds such as synthetic insecticides, e.g., azamethiphos, without any noticeable alteration of its physicochemical characteristics. The study of the release of azamethiphos encapsulated has evidenced a diffusion-controlled profile in agreement with previous studies using

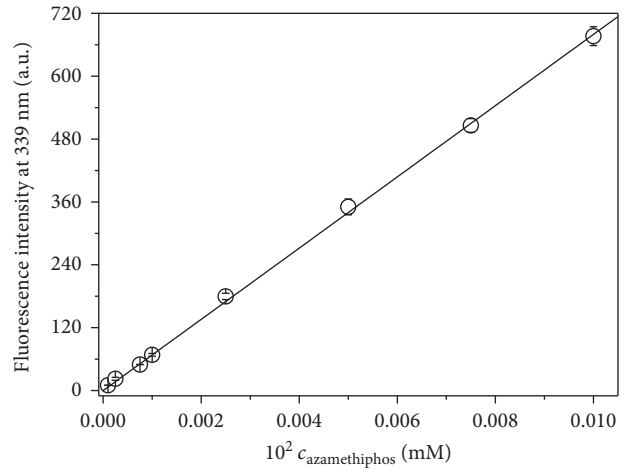

Figure 6: Fluorescence intensity for azamethiphos solutions of different concentrations. The symbols represent the experimental data and the line fitting to the relationship $I = Kc_{azamethiphos}$.

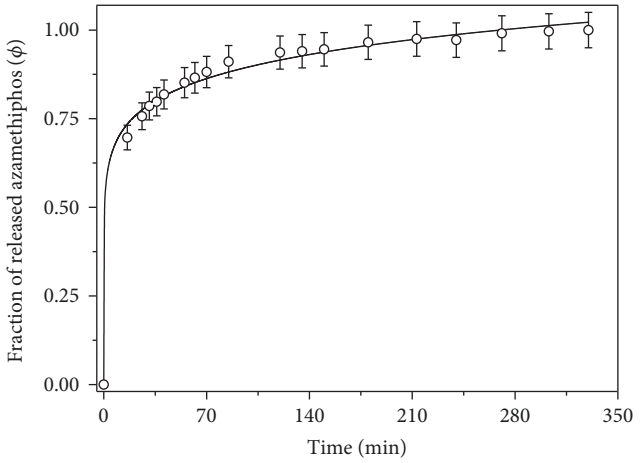

Figure 7: Release kinetics for azamethiphos from agarose nanoparticles represented as the time dependence of the fraction of azamethiphos released from the particles ϕ. The symbols represent the experimental data and the solid lines the fit to the experimental model described by equation (3).

agarose particles. This work offers a new possibility for designing sketched vectors for controlling parasites in water reservoirs. However, further developments of this work require designing methodologies for a better control of the release profile of the encapsulated compounds to provide the bases for a sustained release.

Data Availability

No data were used to support this study.

Disclosure

Pablo G. Argudo's current address is Departamento de Química Física, Universidad de Córdoba, Campus Rabanales, Ed. Marie Curie, 14014 Córdoba, Spain.

Conflicts of Interest

The authors declare that they have no conflicts of interest.

Acknowledgments

PGA, EG, RGR, and FO were funded by MINECO under grant CTQ2016-78895-R, and AL was supported by Agencia Nacional de Promoción Científica y Tecnológica (ANPCyT) PICT 2016-1111. We are grateful to C.A.I. Espectroscopia from the UCM for the use of their facilities.

References

[1] M. A. Augustin and Y. Hemar, "Nano- and micro-structured assemblies for encapsulation of food ingredients," *Chemical Society Reviews*, vol. 38, no. 4, pp. 902–912, 2009.

[2] A. Lucia, A. C. Toloza, E. Guzmán, F. Ortega, and R. G. Rubio, "Novel polymeric micelles for insect pest control: encapsulation of essential oil monoterpenes inside a triblock copolymer shell for head lice control," *PeerJ*, vol. 5, article e3171, 2017.

[3] E. Guzmán, A. Mateos-Maroto, M. Ruano, F. Ortega, and R. G. Rubio, "Layer-by-layer polyelectrolyte assemblies for encapsulation and release of active compounds," *Advances in Colloid and Interface Science*, vol. 249, pp. 290–307, 2017.

[4] V. Nedovic, A. Kalusevic, V. Manojlovic, S. Levic, and B. Bugarski, "An overview of encapsulation technologies for food applications," *Procedia Food Science*, vol. 1, pp. 1806–1815, 2011.

[5] E. Guzman, R. Chulia-Jordan, F. Ortega, and R. G. Rubio, "Influence of the percentage of acetylation on the assembly of LbL multilayers of poly(acrylic acid) and chitosan," *Physical Chemistry Chemical Physics*, vol. 13, no. 40, pp. 18200–18207, 2011.

[6] B. F. Gibbs, S. Kermasha, I. Alli, and C. N. Mulligan, "Encapsulation in the food industry: a review," *International Journal of Food Sciences and Nutrition*, vol. 50, no. 3, pp. 213–224, 1999.

[7] E. Guzmán, J. A. Cavallo, R. Chuliá-Jordán et al., "pH-induced changes in the fabrication of multilayers of poly(acrylic acid) and chitosan: fabrication, properties, and tests as a drug storage and delivery system," *Langmuir*, vol. 27, no. 11, pp. 6836–6845, 2011.

[8] A. Madene, M. Jacquot, J. Scher, and S. Desobry, "Flavour encapsulation and controlled release–a review," *International Journal of Food Science & Technology*, vol. 41, pp. 1–21, 2006.

[9] A. Lucia, P. G. Argudo, E. Guzmán, R. G. Rubio, and F. Ortega, "Formation of surfactant free microemulsions in the ternary system water/eugenol/ethanol," *Colloids and Surfaces A: Physicochemical and Engineering Aspects*, vol. 521, pp. 133–140, 2017.

[10] G. A. Reineccius, "Role of carbohydrates in flavor encapsulation," *Journal of Dairy Science*, vol. 45, pp. 144–146, 1991.

[11] T. A. Tari and R. S. Singhal, "Starch based spherical aggregates: reconfirmation of the role of amylose on the stability of a model flavouring compound, vanillin," *Carbohydrate Polymers*, vol. 50, no. 3, pp. 279–282, 2002.

[12] B. K. Green and L. Scheicher, "Pressure sensitive record materials," US Patent 2,712,507, 1955, NCR Corp USA.

[13] R.-S. Liu, Ed., *Controlled Nanofabrication: Advances and Applications*, Pan Stanford Publishing, Boca Raton, FL, USA, 2013.

[14] Y. Wang, P. Li, T. T.-D. Tran, J. Zhang, and L. Kong, "Manufacturing techniques and surface engineering of polymer based nanoparticles for targeted drug delivery to cancer," *Nanomaterials*, vol. 6, no. 2, p. 26, 2016.

[15] J. P. Rao and K. E. Geckeler, "Polymer nanoparticles: preparation techniques and size-control parameters," *Progress in Polymer Science*, vol. 36, no. 7, pp. 887–913, 2011.

[16] S. Nitta and K. Numata, "Biopolymer-based nanoparticles for drug/gene delivery and tissue engineering," *International Journal of Molecular Sciences*, vol. 14, no. 1, pp. 1629–1654, 2013.

[17] O. G. Jones and D. J. McClements, "Functional biopolymer particles: design, fabrication, and applications," *Comprehensive Reviews in Food Science and Food Safety*, vol. 9, no. 4, pp. 374–397, 2010.

[18] A. Matalanis, O. G. Jones, and D. J. McClements, "Structured biopolymer-based delivery systems for encapsulation, protection, and release of lipophilic compounds," *Food Hydrocolloids*, vol. 25, no. 8, pp. 1865–1880, 2011.

[19] I. J. Joye and D. J. McClements, "Biopolymer-based nanoparticles and microparticles: fabrication, characterization, and application," *Current Opinion in Colloid & Interface Science*, vol. 19, no. 5, pp. 417–427, 2014.

[20] C. P. Reis, R. J. Neufeld, S. Vilela, A. J. Ribeiro, and F. Veiga, "Review and current status of emulsion/dispersion technology using an internal gelation process for the design of alginate particles," *Journal of Microencapsulation*, vol. 23, no. 3, pp. 245–257, 2006.

[21] L. Chen and M. Subirade, "Alginate–whey protein granular microspheres as oral delivery vehicles for bioactive compounds," *Biomaterials*, vol. 27, no. 26, pp. 4646–4654, 2006.

[22] T. Heidebach, P. Först, and U. Kulozik, "Microencapsulation of probiotic cells by means of rennet-gelation of milk proteins," *Food Hydrocolloids*, vol. 23, no. 7, pp. 1670–1677, 2009.

[23] M. R. Saboktakin, R. M. Tabatabaee, A. Maharramov, and M. A. Ramazanov, "Design and characterization of chitosan nanoparticles as delivery systems for paclitaxel," *Carbohydrate Polymers*, vol. 82, no. 2, pp. 466–471, 2010.

[24] S. Salatin, J. Barar, M. Barzegar-Jalali, K. Adibkia, M. A. Milani, and M. Jelvehgari, "Hydrogel nanoparticles and nanocomposites for nasal drug/vaccine delivery," *Archives of Pharmacal Research*, vol. 39, no. 9, pp. 1181–1192, 2016.

[25] R. Satar, S. A. Iizhar, M. Rasool, P. N. Pushparaj, and S. A. Ansari, "Investigating the antibacterial potential of agarose nanoparticles synthesized by nanoprecipitation technology," *Polish Journal of Chemical Technology*, vol. 18, no. 2, pp. 9–12, 2016.

[26] N. Wang and X. S. Wu, "Preparation and characterization of agarose hydrogel nanoparticles for protein and peptide drug delivery," *Pharmaceutical Development and Technology*, vol. 2, no. 2, pp. 135–142, 1997.

[27] S. Ansari, S. Ahmad, M. Jafri, M. Naseer, and R. Satar, "Utility of functionalized agarose nanoparticles in hydrolyzing lactose in batch reactors for dairy industries," *Química Nova*, vol. 41, pp. 429–433, 2018.

[28] V. Kattumuri, M. Chandrasekhar, S. Guha et al., "Agarose-stabilized gold nanoparticles for surface-enhanced Raman spectroscopic detection of DNA nucleosides," *Applied Physics Letters*, vol. 88, no. 15, article 153114, 2006.

[29] H. Hassanvand and P. Hashemi, "Synthesis of silver nanoparticles–agarose composite and its application to the optical detection of cyanide ion," *Analytical Sciences*, vol. 34, no. 5, pp. 567–570, 2018.

[30] S. Talegaonkar, A. Azeem, F. Ahmad, R. Khar, S. Pathan, and Z. Khan, "Microemulsions: a novel approach to enhanced drug delivery," *Recent Patents on Drug Delivery & Formulation*, vol. 2, no. 3, pp. 238–257, 2008.

[31] Z. Wang, K. Yang, H. Li et al., "In situ observation of sol-gel transition of agarose aqueous solution by fluorescence measurement," *International Journal of Biological Macromolecules*, vol. 112, pp. 803–808, 2018.

[32] R. Medina-Esquivel, Y. Freile-Pelegrin, P. Quintana-Owen, J. M. Yáñez-Limón, and J. J. Alvarado-Gil, "Measurement of the sol–gel transition temperature in agar," *International Journal of Thermophysics*, vol. 29, no. 6, pp. 2036–2045, 2008.

[33] B. T. Hargrave, Ed., *Environmental Effects of Marine Finfish Aquaculture*, Springer, Berlin, Heidelberg, 2005.

[34] G. Giammona, F. Goffredi, V. Turco Liveri, and G. Vassallo, "Water structure in water/AOT/*n*-heptane microemulsions by FT-IR spectroscopy," *Journal of Colloid and Interface Science*, vol. 154, no. 2, pp. 411–415, 1992.

[35] M. Goffredi, V. T. Liveri, and G. Vassallo, "Refractive index of water-AOT-*n*-heptane microemulsions," *Journal of Solution Chemistry*, vol. 22, no. 10, pp. 941–949, 1993.

[36] E. Negro, R. Latsuzbaia, A. H. de Vries, and G. J. M. Koper, "Experimental and molecular dynamics characterization of dense microemulsion systems: morphology, conductivity and SAXS," *Soft Matter*, vol. 10, no. 43, pp. 8685–8697, 2014.

[37] E. I. Franses and T. J. Hart, "Phase behavior and molecular motion of aerosol OT in liquid-crystalline phases with water," *Journal of Colloid and Interface Science*, vol. 94, no. 1, pp. 1–13, 1983.

[38] P. Serwer, "Agarose gels: properties and use for electrophoresis," *Electrophoresis*, vol. 4, no. 6, pp. 375–382, 1983.

[39] C. Rochas, A. Hecht, and E. Geissler, "Swelling properties of agarose gels," *Journal de Chimie Physique*, vol. 93, pp. 850–857, 1996.

[40] M. J. Taylor, P. Tomlins, and T. S. Sahota, "Thermoresponsive gels," *Gels*, vol. 3, no. 1, p. 4, 2017.

[41] N. A. Peppas, P. Bures, W. Leobandung, and H. Ichikawa, "Hydrogels in pharmaceutical formulations," *European Journal of Pharmaceutics and Biopharmaceutics*, vol. 50, no. 1, pp. 27–46, 2000.

[42] J. Siepmann and N. A. Peppas, "Modeling of drug release from delivery systems based on hydroxypropyl methylcellulose (HPMC)," *Advanced Drug Delivery Reviews*, vol. 48, no. 2-3, pp. 139–157, 2001.

[43] M. R. Rekha and C. P. Sharma, "Synthesis and evaluation of lauryl succinyl chitosan particles towards oral insulin delivery and absorption," *Journal of Controlled Release*, vol. 135, no. 2, pp. 144–151, 2009.

[44] A. Sosnik, "Alginate particles as platform for drug delivery by the oral route: state-of-the-art," *ISRN Pharmaceutics*, vol. 2014, Article ID 926157, 17 pages, 2014.